Water Cooled Induction Traction Motor for 100 % Low Floor Tram Car

Pavel Dvořák¹⁾, Tomáš Fajt²⁾, Iva Sošková³⁾ and Jakub Hloužek⁴⁾

¹⁾ ŠKODA ELECTRIC a.s., Plzeň, Czech Republic, e-mail: pavel.dvorak@skoda.cz

²⁾ ŠKODA ELECTRIC a.s., Plzeň, Czech Republic, e-mail: tomas.fajt@skoda.cz

³⁾ TechSoft Engineering, spol. s r.o., Praha, Czech Republic, e-mail: soskova@techsoft-endg.cz

⁴⁾ TechSoft Engineering, spol. s r.o., Praha, Czech Republic, e-mail: *hlouzek@techsoft-endg.cz*

Abstract — The paper deals with the design of the traction motor for 100 % low floor tram car. Within the design it was necessary to deal with many problems which have significant impact on the final product. The most interesting problems were the conception of the torque transmission, mounting of the brake equipment on the motor body, arrangement of the motor inside the bogie, cooling of the motor or protection of the motor against the water and pollution which can enter inside the motor. In this paper there are discussed the electromagnetic model, and special thermal and ventilation model of the motor. The final design was validated within the type testing.

Keywords: induction traction motor, tram car, electromagnetic field, temperature field, ventilation circuit, equivalent circuit.

I. INTRODUCTION

Traction induction motors are the most popular and they are used in many electric vehicles. Most vehicles of the city transport will be low floor for easy entry and exit of passengers. Regarding to this requirement, construction of the vehicle bogie and traction drive must be small and compact.

Fig. 1. Illustration of the tram-car bogie.

This paper deals with the design aspects of the traction motor for a tram-car. The described traction motor is induction, squirrel cage motor and it is water cooled. The traction motor is mounted outside of the bogie (see Fig. 1) and it is connected with a gear box.

II. DESCRIPTION OF THE TRACTION MOTOR

Nowadays, the design of an induction motor is not difficult discipline. On the other hand, requirements which are necessary to be fulfilled are often very rigorous. Due to this the design of the motor is very difficult and problematic. At the beginning it is necessary to calculate, that the environment conditions and position of the motor in the bogie plays a major role. The motor can be exposed in the operation to various pollutions and therefore it needs to be adequately protected.



Fig. 2. View to the traction motor.

Another aspect influencing the design of the traction motor is its size. Necessity of the motor compact dimensions together with torque requirements has an effect on the size of the magnetic circuit, its saturation and cooling. All these requirements lead to a closed compact liquid-cooled traction motor.

III. DESIGN OF THE TRACTION MOTOR

A. Electrimagnetic model of the traction motor

The electromagnetic model can be prepared with analogy between magnetic and electric circuit. In this case the magnetic flux corresponds to electric current and reluctance corresponds to electric resistance. The magnetic circuit can be replaced by an electric circuit which can be solved by standard methods.

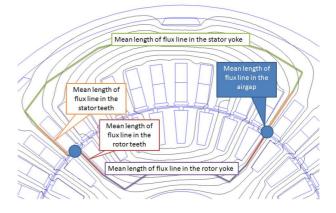


Fig. 3. Flux lines in the motor cross-section .

The model of the motor can be reduced to one pair of poles (see Fig. 3). In this figure there are illustrated flux lines and there can be seen one pair of poles in the magnetic circuit.

The calculation method is based on analytical formulas [5] and it uses vast range of simplification aspects and it is suitable in first stage of the design. The simplification is in symmetrical magnetic circuit (only circular outer perimeter is enabled) and/or the field intensity in several parts of the magnetic circuit is considered to be constant, etc...

Main advantage of this method is quickness of obtaining first results. The results from first stage of the design can be used for optimization by a suitable numerical method. In present, the most popular is the finite element method (FEM). Basis of FEM is partition of the geometry of the motor to a finite number of the triangles (in 2D) or tetrahedrons (in 3D).

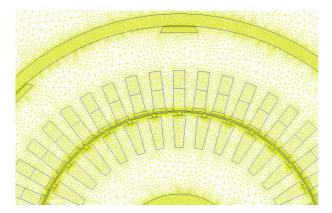


Fig. 4. Illustration of the 2D triangle mesh.

In Fig. 4 there is shown the 2D triangle mesh of the motor cross section. For acceleration of the solution in the finite element analysis (FEA) geometrical symmetry may be also considered and used. Computation of next characteristic values is relatively simple.

B. Equivalent circuit

For analysis and control of the motor it is necessary to define values of the equivalent circuit (see Fig. 5). This circuit is basis of the mathematical model of the control algorithm.

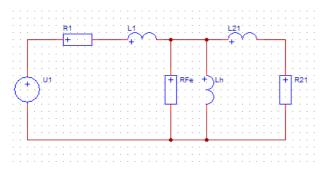


Fig. 5. Full equivalent circuit of the induction motor.

Main circuit parameters are winding resistance of the stator (R_1) and rotor (R_{21}) , leakage inductance of the stator (L_1) and rotor (L_{21}) , main inductance (L_h) and core resistance (R_{Fe}) . All of these values are possible to be obtained from calculation and then to be adjusted after

testing. Accuracy of the prediction of equivalent circuit parameters is necessary for minimization of further errors with bad mathematical model.

C. No-Load operation

This operation is characterised by the rotor synchronous speed. The slip is close to zero, therefore the rotor resistance R_{21} is much bigger than R_{Fe} and the equivalent circuit will have a new topology (see Fig. 6).

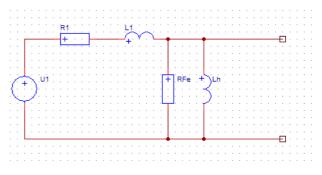


Fig. 6. Equivalent circuit in no-load operation.

The distribution of the flux density in the motor crosssection gives information about saturation of the magnetic circuit (see Fig. 7).

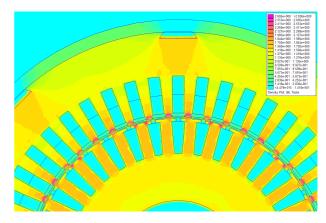


Fig. 7. Distribution of the flux density in the motor cross-section .

Difference between analytical and numerical solution of the magnetic flux density is very small (see Table I).

 TABLE I.

 COMPARISON OF ANALYTICAL AND FEM RESULTS

	flux density B (T) in stator		flux density B (T) in rotor	
placement	analytical	FEM	analytical	FEM
yoke	1.5	1.6	1.4	1.4
teeth	1.6	1.7	1.9	1.7

The magnetic flux and terminal voltage dependency on no-load current gives magnetization characteristic. In Fig. 8 it is possible to compare the magnetisation characteristics.

No load operation gives information about the value of the stator current, losses, main inductance and core resistance.

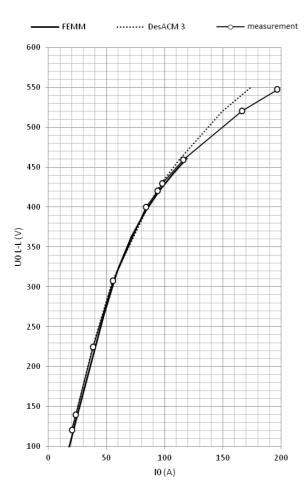


Fig. 8. Magnetisation characteristic.

D. Locked rotor operation

This operation is characterised by the blocked rotor – the slip is close to 1. The rotor resistance R_{21} is small compared to R_{Fe} and the equivalent circuit will have a new topology (see Fig. 9).

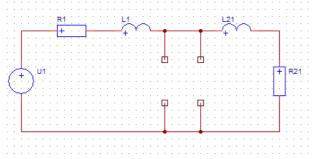


Fig. 9. Equivalent circuit in locked rotor operation.

This operation gives information about the leakage inductance $(L_1 + L_{21})$ and resistance $(R_1 + R_{21})$. The slip is equal 1, frequency of the rotor field equals with the stator frequency and the skin-effect in the rotor must be considered.

For dividing the leakage inductance to stator and rotor value it is suitable to use the ratio L_1 / L_{21} from the analytical design. For the analysed motor this ratio is about 1.2.

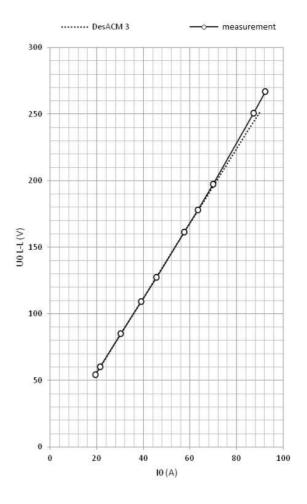


Fig. 10. Locked rotor characteristic.

E. Nominal loading

The traction motor is loaded by nominal torque (Nm) and speed (rpm). This operation is maintained till stator winding temperature reaches steady state. For steady state temperature it may be considered a condition where the temperature varies no more than 2 K per hour [3]. After that, values of stator resistance, frequency, power losses and power factor may be measured.

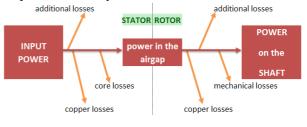


Fig. 11. Losses distribution.

Based on all parameters from the no-load, locked rotor and nominal loading operation it is possible to make distribution of losses in the motor (see Fig. 11).

In Table II there are recorded the most important parameters of the motor. Calculation of the electric parameters was referenced to temperatures extracted from the measurement. In Table III there are stored parameters of equivalent circuit (see Fig. 5) of the motor referenced to 20 °C. In both of tables the values named (M) are measured and values named (C) are calculated values. Regarding the values, the model gives quite good results.

name	unit	calculation (C)	measure. (M)	M vs C (%)
power output	kW	100	100.3	0.3
speed	rpm	2217.5	2218.4	0.04
L-L voltage	V	420	420.6	0.15
phase current	А	178.3	177.8	-0.28
frequency	Hz	75	75	0
total losses	kW	8.6	8.5	-0.5
power factor	-	0.84	0.84	0
stator winding temperature rise	К	70	68	-2.94
water temperature	°C	60	60	0
Slip (hot)	%	1.44	1.42	-1.83
power in the air gap	kW	101.5	101.7	0.27
mechanical losses	W	87.4	120	27.2
Cu losses – stator	W	2948.4	2562.2	-15.1
Cu losses – rotor	W	2166.2	1322.7	-63.8
core losses	W	862	1537	43.9
add. losses	W	2372.2	2965.8	20

 TABLE II.

 COMPARISON OF ANALYTICAL AND MEASUREMENT RESULTS

TABLE III. Comparison of analytical and measurement results – equivalent circuit parameters

name	unit	calculation (C)	measure. (M)	M vs C (%)
R_1	mΩ	20.3	19	-7
<i>R</i> ₂₁	mΩ	14	14	0
L_1	mH	0.23	0.235	2.2
L_{21}	mH	0.192	0.196	2.2
L _h	mH	5.623	5.483	-2.6
R _{Fe}	Ω	46	70.6	34.8

Temperature of the stator and rotor winding has very significant impact on parameters of the motor mathematical model .Good estimation plays important role for the motor control. For this it was created a ventilation and thermal model of the analyzed motor.

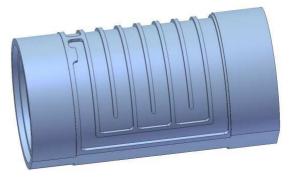


Fig. 12. Illustration of the water channel.

IV. VENTILATION AND THERMAL DESIGN

Liquid is considered as a most efficient coolant. Liquid – water cooling was chosen for cooling of the analyzed motor. Due to this, the construction of the motor may be very compact instead of self air ventilation. In case of self ventilation the length of the motor depends on dimensions of the ventilator. Also from the noise point of view the water cooled motors are less noisy than self air ventilated motors. Advantage of water cooling is in the better possibility for assembly of the motor with the bogie (see Fig. 1). Regarding to this the cooling via water channel placed on outer perimeter of the stator was chosen (see Fig. 12).

Thanks to this, the stator is more actively cooled than rotor and it brings some problems with cooling of other motor parts (rotor winding, bearings, etc.). Due to the stator frame, the next problem was impossibility to use whole area of the stator lamination for cooling (see lower part of the stator frame in Fig. 12).

Coolant flow quantity was defined based on calculation to 20 l/min and work temperature of the water on the inlet is 60 $^{\circ}$ C.

The method of the ventilation and thermal equivalent net (VTE net) and method are based on numerical calculations (CFD) in the computer program of ANSYS Fluent. These methods were used for the ventilation and thermal calculation of the analyzed traction motor.

Both methods of calculation use as input parameter the distribution of the losses in the motor based on a electromagnetic calculation. In the thermal calculation the heat transfer by conduction and heat transfer by convection were considered between the solids and liquid.

A. Ventilation and thermal equivalent net (VTE net)

This method is based on the equivalent net which consists of the heat sources, thermal nodes and places of heat dissipation. These elements are connected to each other with thermal resistances.

The method is very simple, fast and universal. Therefore it can be used also in case of the motor 3D model not done yet. Results of the analysis by this method are known within several minutes. For the analysis it was used the universal thermal model of the water-cooled motor. This model is a standard model used for such types of the motor of the SKODA ELECTRIC a.s. production.

The model of the motor is possible into divide to two parts. First is the ventilation. The ventilation calculation for water-cooled motor gives information about the pressure drop of the cooling channel and defines average of the water velocity. The pressure drop calculation is based on definition of the ventilation resistance of each parts of the water channel. Result of the calculation is the pressure drop (25 kPa) for the defined water flow quantity (20 l/min). Average water velocity is 0.9 m/s.

Second is the thermal calculation. Aim of the solution is to define the temperature of monitored nodes of the thermal net. As input there are losses, boundary conditions (altitude, ambient temperature, inlet water temperature and speed of the rotor). As result of the analysis there are the average temperature rise of the stator winding (66 K), temperature rise of the water (5.9 K) and maximum temperature of bearings (108 °C).

B. CFD method

The CFD method is possible to be used with a real 3D model of the traction motor (see Fig.13). However, for the CFD analysis it is necessary to modify the real 3D model. Some details in geometry which has no influence on the main problem (water flow) will be deleted or modified. These modifications were done with help of the ANSYS DesignModeller and ANSYS SpaceClaim programs.

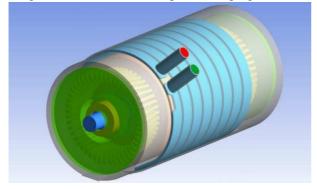


Fig. 13. Computer model of the traction motor geometry.

The mesh for the calculation (see Fig. 14) was created by the ANSYS Meshing. The problem of water flow was defined as an incompressible, viscous and turbulent [4]. For the complete model the inner air flow was considered. This air flow was caused by the rotor rotation.

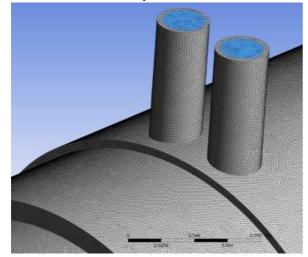


Fig. 14. The zoom to mesh.

This analysis was done with help of the TechSoft Engineering Company, which did all of the CFD analysis.

Based on the ventilation simulation (see Fig. 15) of water flow inside the water channel it was defined its pressure drop (19.5 kPa) for water flow quantity (20 l/min).

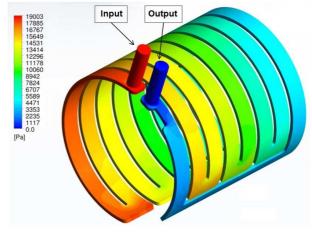


Fig. 15. Pressure field of the water inside water channel.

Together, places were found where the water flow is not good (see Fig. 16). Also places with worst cooling efficiency were found

The result of the thermal analysis gives information about temperatures of all parts of the motor and water inside the water channel. The places with high temperatures which were predicted before analysis were confirmed. The highest temperatures about 230 °C were identified near middle of the rotor cage, rotor lamination and shaft – also in the area of losses formation, which is far from the cooling channel. The stator winding is also significantly warm place, especially its front parts.

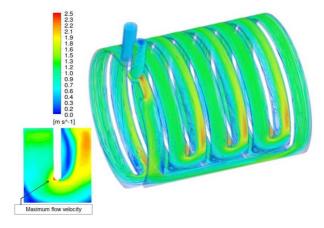


Fig. 16. Water flow in the water channell.

From the calculation on the 3D geometric model it is possible to see the temperature distribution in all parts of the motor (see Fig 17). Especially it is possible to analyze the stator winding temperature (see Fig. 18). The warmest area of the stator winding is on the bottom, where is no cooling (compare with Fig. 12).

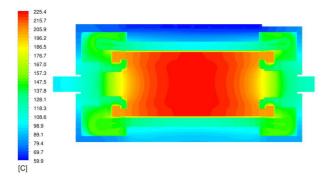


Fig. 17. Temperature distribution in the longitudinal section of the motor.

The average temperature rise of the stator winding is 73 K and the maximum temperature of the front parts of the stator winding is 155 $^{\circ}$ C. The reason of this value is the nonsymmetric cooling channel and rotation of air heated to high temperature inside the motor, which is in contact with the front parts of the stator winding.

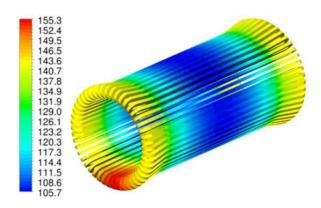


Fig. 18. Temperature distribution of the stator winding.

It was calculated the temperature distribution of the water inside the water channel (see Fig. 19). The total temperature rise of the water is 5.8 K.

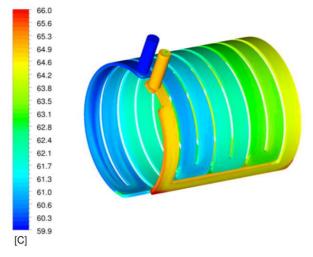


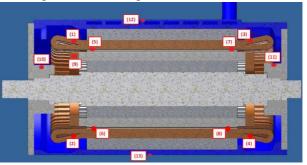
Fig. 19. Temperature distribution of the water.

The results of the simulation gives information, that most problematic parts are bearings. It was confirmed, the

temperature of bearings is more than 120 °C. Therefore the better and more detailed bearings model may be considered. After that, the results of the simulation gives lower values.

C. Comparison of methods

Each simulation is necessary to proof and compare with the measurement on a real motor prototype. This step is most important in case of problematic solution.



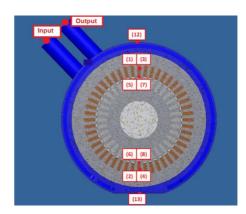


Fig. 20. Specification of points for temperature measurement.

During prototype production places for location of Pt cells were specified (see Fig. 20). In these places the temperature was measured and its value recorded.

In tables (see Table III and Table IV) there is comparison of calculated values from the VTE net and CFD analysis with values from measurement.

TABLE IV. COMPARISON OF CALCULATIONS

Values are in (K)	ventilation and thermal equivalent net	CFD	measurement	comparison between CFD and measurement
average temperature rise of stator winding	66	73	68	7.4

TABLE V.

COMPARISON OF CALCULATIONS

COMPARISON OF CHECOLATIONS						
Placement (see Fig. 20) - (°C)	ventilation and thermal equivalent net	CFD	measurement	comparison between CFD and measurement		
1	145	134	139	-3.6		
2	145	145	142	2.1		
3	144	134	131	2.3		
4	144	145	134	8.2		
5	-	136	135	0.7		
6	-	144	140	2.9		
7	-	136	141	-3.5		
8	-	144	144	0.0		
9	193	182	181	0.6		
10	103	117	91	28.6		
11	108	126	98	28.6		
12	66	64	66	-3.0		
13	13 66		13 66		77	15.6
inlet	60	60	60	0		
outlet	65.9	65.8	65.5	0.5		

There is good conformity between the measurement and calculation. Both simulation methods used simplified bearing model, therefore the maximum differences of the temperature are in location of bearings.

V. CONCLUSION

The electromagnetic, thermal and ventilation model of the closed, water cooled, squirrel cage induction traction motor was defined. Based on the design procedure the real prototype of the motor was created. On the prototype motor there were done the measurements and the used models were checked. Based on measurement results the design methods were slightly modified and they are used for design of further traction motors for another projects realised in SKODA ELECTRIC a.s.

REFERENCES

- I. P. Kopylov, and col., Stavba elektrických strojů, Praha: SNTL, 1988. ISBN-04-532-88.
- K. Hruška, Určení parametrů náhradního schématu asynchronního stroje v programu FEMM. Plzeň, 2008.
- [3] ČSN EN 60342-2, ed. 2: 2011
- [4] ANSYS Fluent 14.5 manuals and help
- [5] J. Pyrhönen T. Jokinen, V. Hrabovcová, *Design of rotating electrical machines*, John Wiley & Sons, Ltd, 2008. ISBN-978-0-470-69516-6